Artificial Muscle Technology: Physical Principles and Naval Prospects

John D. Madden, Nate Vandesteeg, Peter G. Madden, Arash Takshi, Rachel Zimet, Patrick A. Anquetil, Serge R. Lafontaine, Paul A. Wierenga and Ian W. Hunter

***Abstract*—Hydrodynamic understanding of the advantages of unsteady flow and locomotion in fish and insects is creating a demand for bio-mimetic actuator technologies. New actuator materials that employ voltage, field or temperature driven dimensional changes to produce forces and displacements are suggesting new approaches to propulsion and maneuverability. Fundamental properties of these new materials are presented, and examples of potential undersea applications are examined in order to assist those involved in hydrodynamic design and in actuator research to evaluate the current status and developing potential of these artificial muscle technologies. Technologies described are based on newly explored material properties developed over the past decade, and also on older materials whose properties are not widely known. The materials are dielectric elastomers, ferroelectric polymers, liquid crystal elastomers, giant magnetostrictive materials, thermal & ferroelectric shape memory alloys, ionic polymer/metal composites, conducting polymers and carbon nanotubes.**

I. Introduction

This review begins with a description of each actuator technology in sequence. Fundamental mechanisms, basic properties, synthesis, fabrication and applications are presented. For each material a table of properties is presented including:

Stress is the typical or maximum force per cross-sectional area that a given material is able to work against. In all the actuator technologies described, force developed scales linearly with cross-sectional area (whose surface normal is parallel to the direction in which actuation is occurring).

Strain represents the displacement normalized by the original material length in the direction of actuation.

Strain rate is average rate change in strain per unit time during an actuator stroke.

Work Density is the amount of work generated in one actuator cycle per unit volume of actuator. It is very important to note that this does not include the volume occupied by electrolytes, counter electrodes, power supplies, or packaging, unless othersise noted. The reason is that these other aspects do not always scale linearly with volume.

Power to Mass Ratio is the peak power output per unit mass of actuator material (again only the material itself).

Coupling is the proportion of input energy that is transformed into external work. This usually represents a best case, where the output load is perfectly matched to the actuator stiffness, maximizing output.

Efficiency is the ratio of work generated to input energy expended. It can be higher than the coupling because in some cases electrical and thermal energy can be recovered from the actuator e.g. during capacitive discharge. Warning: the listed efficiency has not always been achieved in practice, and sometimes requires additional circuitry to achieve.

Cycle Life is the number of useful strokes that the material is known to be able to undergo before either the actuator performance was significantly degraded or, in some cases, the test was stopped. Cycle life is often highly strain and stress dependent, and sometimes magnitudes of these are not reported in the original work.

Elastic Modulus is the material stiffness normalized by sample length and cross-sectional area. It is important as it determines the actuator's passive ability to reject load changes and disturbances, and along with the mass determines the resonant frequency. Many of these materials are viscoelastic, and therefore creep and stress relaxation are important (but seldom characterized). Some also change stiffness with changing phase or state (usually described by the maximum and minimum moduli).

References relevant to each technology follow its description. Following the descriptions are two case studies presenting basic design calculations relevant to the use of artificial muscle technologies to vary propeller blade camber (static) and to increase thrust by generating unsteady flow conditions.

Previous reviews include:

1. A chapter describing classical actuator technologies (electro-magnetic actuators, combustion engines, hydraulics, piezo-ceramics, muscle) by J. Hollerbach, I. Hunter & J. Ballantyne, "A comparative analysis of actuator technologies for robotics", O. Khatib, J. Craig & Lozano-Perez Eds, *The Robotics Review* 2, MIT Press, Cambridge MA 1992, pp. 299-342.
2. A review of emerging actuator technologies in comparison with muscle written over a decade ago

Manuscript received July 30, 2003. This work was supported in part by the Office of Naval Research grant N00014-1-02-0078.

J. Madden is with the University of British Columbia, Vancouver, Canada (604-827-3506; fax: 604-822-5949; e-mail: jmadden@ ece.ubc.ca). A. Takshi and P. Wierenga are also with the University of British Columbia.

N. Vandesteeg, P. Madden, R. Zimet, S. Lafontaine and I. Hunter are with the BioInstrumentation Laboratory at MIT in Cambridge MA 02139, USA.

but still very relevant. I. Hunter & S. Lafontaine, "A comparison of muscle with artificial actuators", *Technical Digest IEEE Solid State Sensors & Actuators Workshop*, 1992, pp. 178-185.

3. A book with chapters describing many of the technologies presented here edited by Yoseph Bar-Cohen, *Electroactive Polymer (EAP) Actuators as Artificial Muscles - Reality, Potential and Challenges*, SPIE Press, 2001.
4. Proceedings of the SPIE annual Smart Structures and Materials Symposium, which features sessions on Electro-active Polymers, Ferroelectrics and Ferroelectric Shape Memory Alloys.
5. A detailed description of muscle mechanisms and properties is presented by Peter Kohl as part of this conference.
6. Papers by Ashby and colleagues including Huber, J., Fleck, N.A. and Ashby, M.F. 'The selection of mechanical actuators based on performance indices' in *Proc. R. Soc. Lond. A*, **453**, 1997, 2185-2205.
7. WorldWide Electroactive Polymer Actuators Webhub maintained by Y. Bar-Cohen, provides updates on activities and a list of researchers and corporations: http://ndeaa.jpl.nasa.gov/nasa-nde/lommas/eap/EAP-web.htm .

II. Actuator Descriptions

A. Muscle and Biological Actuators

Muscle is a linear actuator technology whose properties, though surpassed in many respects by artificial actuators, is very well suited to providing intermittent displacements and adaptable stiffness in organisms ranging in size from the micrometer scale up to meters in length. Details of the mechanisms are provided by Peter Kohl later in the proceedings. The properties vary by species, as described by Robert Full and Kenneth Meijer, "Metrics of natural muscle." In *Electro Active Polymers (EAP) as Artificial Muscles, Reality Potential and Challenges*, ed. Y. Bar-Cohen, 67-83. SPIE Press 2001. Key properties of mammalian skeletal muscle are provided in Table I for ready comparison with other technologies.

TABLE I
MAMMALIAN SKELETAL MUSCLE [HUNTER & LAFONTAINE 1992]

PROPERTY	TYPICAL	MAXIMUM
Strain (%)	20	> 40
Stress (MPa)	0.1 (sustainable)	0.35
Energy Density (kJ·m^{-3})	0.8	
Density (kg·m^{-3})	1037	
Strain Rate (%·s^{-1})		500
Power to Mass (W·kg^{-1})	50	200
Efficiency (%)		40
Cycle Life		10^9
Modulus (MPa)	10 - 60	

B. Dielectric Elastomer Actuators

Synonymns: EPAM.

Mechanisms: Electrostatic attraction between conductive layers applied to two surfaces of elastomer films induces compressive strains under applied fields of ~ 100 MV/m. In elastomers the materials are sufficiently compliant that large strains are induced and there is efficient coupling between the electrical energy input and mechanical energy output. Since elastomers maintain constant volume, contraction in one direction leads to expansion in the other two. By pre-straining one of the other two axes, all expansion is directed into the one direction.

Features: Elegantly simple in mechanism and construction. Large strains (~100 %) and good frequency response (~ 1 kHz). Good efficiencies, especially when energy is recovered (60 %). Can act as a generator.

TABLE II
DIELECTRIC ELASTOMERS [1,2,3]

PROPERTY	SILICONE	VHB
Strain (%)	100	200
Stress (MPa)	0.4-0.8	2.4
Energy (kJ/m^3)	1.6	58
Density (kg/m^3)	1100	960
Strain Rate (%/s)	327600	3010
Power (W/kg)	750	3400
Bandwidth (Hz)	1400	7
Life (cycles)	10^7	
Coupling (%)	6	54
Efficiency (%)	10	60
Modulus (MPa)	0.35	0.6
Coef. Of Thermal Exp. (m/m/°C)		1.80E-04
Strength (MPa)	6.2	0.690
Voltage (V)	>1000	>1000
Charge (C/m^3)		46
Max. Field (MV/m)	110-350	125-412

Limitations: High voltages (> 1 kV) can be an issue, particularly in biomedical and toy applications. For large and fast devices the power may provide a real hazard. Dielectric breakdown can limit actuator yield particularly when imperfections exist within films. These materials are low in stiffness and exhibit creep, so that although relatively large stresses can be applied (2.4 MPa), operation is more typically at ~ 100 kPa. Generally there is a need to convert line voltages or battery potentials up to kilovolt potentials which adds cost and consumes volume.

Theory: According to the Maxwell stress the polymer is squeezed in Z direction and the stress in Z direction can be derived as:

$$P_z = \varepsilon_r \varepsilon_0 E^2 = \varepsilon_r \varepsilon_0 (V/t)^2 \qquad (1)$$

While P_z is the stress in Z direction ε_r is relative permittivity ε_0 is the free space permittivity, E is the applied electric field V is the applied voltage and t is the thickness of the polymer.

Regarding the equation, to obtain more stress the applied voltage should be increased as much as possible and the thickness of polymer should be the minimum possible value. The maximum stress is limited by dielectric breakdown, which is a function of strain.

The resultant strains produced in the polymer are dependent

on the boundary conditions and loads on the polymers. Further, the strain depends on the elastic modulus of the polymer, which for elastomers at large strains may be nonlinear. Another important point is that usually polymers, which are used, should have a large prestrain in order to get appropriate response. Such a prestrains may be anistropic and cause the effective elastic modulus to be anistropic as well. So it is not easy to write a simple general equation for strain. But considering the incompressibility of polymer, gives the same volume when it is squeezed so the strain in the thickness S_z may be related to the in plane strains S_x and S_y as:

$$(1+S_x)(1+S_y)(1+S_z) = 1 \qquad (2)$$

Definitely S is the relative strain, which is the strain difference from prestrain conditions.

Rate limiting factors include the inertia of the apparatus, damping within the elastomer film and the RC charging time constant.

Materials and Dimensions: A number of elastomers have been tested (Ref), with the best results have been achieved from three commercially available materials:

1- Dow Corning HS3 silicone
2- Nusil CF 19-2186 silicone
3- 3M VHB 4910 acrylic

The silicones must be cast into the appropriate geometry, while the VHB is purchased as an adhesive ribbon. Typical actuator dimensions before stretching are 100 μm thick, one hundred millimetres long and similar dimensions in width. These films are coated with conductive grease, poweder or paint. Pre-stretching of up to 500 % is performed by rolling films, inserting them into a compliant frame or by using beams to maintain the tension. Voltage is applied to either side at voltages of up to 4 kV and using currents that can reach the milliamp range.

Forces generated to date have reached the ~10 N and displacements reach ~ 100 mm [5].

Key Investigators and Corporations:

Ron Pelrine, Roy Kornbluh and colleagues at SRI, Menlo Park CA. This group initiated the recent work on dielectric elastomers, and continues to be a leader in their characterization and application.

Peter Sommer-Larsen and colleagues at The Technical University of Denmark are doing excellent work characterizing dielectric elastomers.

A number of other groups are applying dielectric elastomers to robotics and medical devices (Steven Dubowsky at MIT), and micro flying insects (Yan and Madden, http://www.ece.ubc.ca/~josephy).

Temperature: Dielectric elastomers have been operated successfully at 150 °C, but little else is known about the temperature dependence of their performance. Operation well below glass transition temperatures is anticipated to be ineffective as their compliance will drop by two or more orders of magnitude.

Applications: Demonstration devices include speakers (tweeters), and robotic legs (ref.).

Potential: Layers of thin films could enable voltage to be substantially reduced. Ideally these layers would be as thin as 100 nm, reducing potentials to the 10 V range.

References:

[1] R.Kornbluh, R.Pelrine, Q. Pei, S. Oh, J. Joseph, "Ultrahigh strain response of field-actuated elastomeric polymers"

[2] G.Kofod "Dielectric Elastomer Actuators" Ph.D. thesis, The Technical University of Denmark, September 2001

[3] P.Sommer-Larsen "Final report about ARTMUS-Artificial Muscles project" Riso National Laboratory, December 2001

[4] P.Sommer-Larsen, G.Kofod, S. MH, M. Benslimane, P. Gravesen, "Performance of dielectic elastomer actuators and materials" Smart Structure and Materials 2002, Electroactive Polymer Actuators and Devices, Proc. SPIE Vol. 4695, pp. 158-166.

[5] R. Perline, R. Kornbluh, Q. Pei, S. Stanford, S. Oh, J. Eckerle, "Dielectric Elastomer Artificial Muscle Actuators: Toward Biomimetic Motion" " Smart Structure and Materials 2002, Electroactive Polymer Actuators and Devices, Proc. SPIE Vol. 4695, pp. 126-137.

[6] M. Benslimane, P. Gravesen, "Mechanical properties of Dielectric Elastomer Actuators with smart metallic compliant electrodes" " Smart Structure and Materials 2002, Electroactive Polymer Actuators and Devices, Proc. SPIE Vol. 4695, pp. 150-157

[7] G. Kofod, R. Kornbluh, R. Pelrine, P. Sommer-Larsen, "Actuation response of polyacrylate dielectric elastomers" Smart Structure and Materials 2001, Electroactive Polymer Actuators and Devices, Proc. SPIE Vol. 4329, pp. 141-147.

[8] R. Pelrine, R. Kornbluh, G. Kofod, "High strain Actuator Materials Based on Dielectric Elastomers" ADVANCED MATERIALS, 12: (16) 1223-1225 AUG 16 2000

[9] R. Pelrine, R. Kornbluh, J. Joseph, S. Chiba "Artificial Muscle for Small Robots" Transactions of the Institute of Electrical Engineers of Japan 2002 Feb. Vol. 122 No.2 pp.97-102.

[10] P.Sommer-Larsen, J. HookerG.Kofod, K. West, M. Benslimane, P. Gravesen, "Response of dielectric elastomer actuators" Smart Structure and Materials 2001, Electroactive Polymer Actuators and Devices, Proc. SPIE Vol. 4329, pp. 157-163.

C. Relaxor Ferroelectric Polymer Actuators

TABLE III
FERROELECTRIC POLYMERS [12,16]

PROPERTY	MIN	TYP	MAX
Strain (%)	0	3.5	5
Stress (MPa)			43
Energy (kJ/m^3)	320		920
Density (kg/m^3)	1870		2000
Strain Rate (%/s) S3			5
Strain Rate (%/s) S1			4.3
Power (W/kg)			
Bandwidth (Hz)		5	100000
Life (cycles)			
Coupling (%) S3			0.3
Coupling (%) S1			0.45
Modulus (MPa)			400
Strength (GPa)			
Voltage (V)			> 1000
Max. Field (MV/m)			150

Overview: The application of an electric field changes the alignment of polar groups on the polymer backbone, resulting in conformational changes and macroscopic deformation.

Features: Moderate strains (up to 5 %), high stresses (reach

45 MPa), good frequency response (~ 100 kHz), large work per cycle of 1 $MJ \cdot m^{-3}$, and good stiffness (~ 0.4 GPa). Synthesis methods are similar to those used for polyethylene, with good potential for mass production.

Limitations: Requires high fields (150 $MV \cdot m^{-1}$) and voltages (> 1 kV) creating the same problems outlined for dielectric elastomers. Some of the fluorocarbons used in the synthesis of the materials are difficult to obtain due to environmental restrictions on their use. The process of irradiation, used in a number of the materials, is expensive and time consuming. Strain is load dependent.

Potential: As with the dielectric elatomers, the high voltage can be reduced by using thin layers (100 nm for 15 V) or materials with very high dielectric constant [Bharti].

Temperature: The Curie Points of many of these materials is just below room temperature. The dielectric constant and the efficiency of coupling electrical and mechanical work is also a function of temperature.

Heat can be used instead of electrostatic energy to activate ferroelectric polymers. Heating and cooling these polymers around their Curie point produces reversible actuation, with the coupling determined by the Carnot efficiency.

Mechanisms: Ferroelectric materials are the electrostatic analogs of ferromagnets. The application of an electric field aligns polarized domains within the material. When the applied field is removed, a permanent polarization remains. As in ferromagnets, ferroelectrics are characterized by a Curie Point, a temperature above which thermal energy prevents permanent polarization.

The ferroelectric polymer most commonly used for actuation is Poly(Vinylidene Fluoride – TriFluoroethylene. The electronegativity of the fluorine makes the polymer backbone highly polar. Local polar groups align to create polarized domains. The application of an electric field aligns polarized domains, which remain even after the field is removed. The realignment also produces reversible conformational changes which are made use of in actuation.

A key disadvantage of ferroelectric polymers is that there is substantial hysteresis. A large field must be applied in the opposite direction of the initial field in order to reverse the polarization, and substantial energy is expended, which does not produce mechanical work. The most successful materials have instead been ferroelectric relaxors in which the long range correlation between polar groups is disrupted by imperfections. These imperfections are either introduced by irradiation [Zhang 2] or by the incorporation of disruptive monomers such as chlorotrifluoroethylene. The resulting polymers are ferroelectric relaxors, becoming paraelectric when field is removed, and displaying minimal hysteresis.

In P(VDF-TrFE) ferroelectric relaxors, application of field leads to a contraction in the direction between plates (S3), and extension perpendicular to the applied field (S1, S2). Pre-straining in one direction – e.g. S2 – enlarges the strain in the other direction – e.g. S1. The enhancement resulting from prestraining may be partly due to material anisotropies that are introduced during stretching.

References:

[11] Zhang, Qiming; Scheinbeim, Jerry, "Electric EAP" in *Electroactive Polymer Actuators as Artificial Muscle*, Y. Bar-Cohen, Ed. Bellingham, Washington: SPIE Press, 2001, pp.89-117.

[12] Zhang, Q. et al, "P(VDF-TrFE)-based Electrostrictive Co/Ter-Polymers and its Device Peformance" in *Electroactive Polymer Actuators and Devices*, Y. Bar-Cohen, Ed. Bellingham, Washington: SPIE Press, 2001, pp. 106-116

[13] Bharti, V. et al, "High Dielectric Constant Composites Based on Metallophthalocyanine Oligomer and Poly(vinylidene fluoride-trifluoroethylene) Copolymer" in *Journ of Applied Polymer Science*, Wiley & Sons, Inc., Vol. 82, 70-75, 2001, Vol. 82, 70-75

[14] Tashiro, K.; Nishimura, S.; Kobayashi, M., "Thermal Contraction and Ferroelectric Phase Transition in Vinylidene Fuoride-Trifluoroethylene Copolymers. 1. An Effect of Tensile Strength along the Chain Axis" in Macromolecules, ACS, 1988, Vol 21, 2463-2469

[15] U.S. Patent # 6,355,749 (Outlines manufacturing. Also gives wide range of values for dielectric constants. Discusses dielectric constant temperature dependence and Curie temperature transition at room temp for terpolymer (a relaxor).

[16] Zhang, Q.M. et al, "Electrostrictive poly(vinylidene fluoride-trifluoroethylene) copolymers", Sensors and Actuators A,, Vol 90, 2001, 138-147

D. Liquid Crystal Elastomers (LCE)

Overview: Thermal or electrostatic energy are employed to induce phase changes in liquid crystalline polymers. The changes in order and alignment of liquid crystalline side chains generates stresses in the polymer backbone, resulting in actuation.

TABLE IV
LIQUID CRYSTAL ELASTOMERS [22,26,28]

PROPERTY	THERMAL	E-FIELD
Strain (%)	40-45	4
Stress (MPa)	0.27	
Energy (kJ/m^3)	56	
Density (kg/m^3)		
Strain Rate (%/s)	37	530
Power (W/kg)	1	
Coupling (%)		
Modulus (MPa)		
Strength (GPa)		
Voltage (V)		0.1125
Max. Field (MV/m)		1.5
Dielectric Constant		

Mechanisms: In 1975 de Gennes predicted that the reorientation of liquid crystal molecules during a phase transition could lead to a mechanical stress and strain. Stress fields in normal liquid crystals generally induce flow that prevents the buildup of a static stress. In liquid crystal elastomers, the free flow of the liquid crystal molecules (mesogens) is prevented by bonding them to a cross-linked polymer where the flexible polymer backbone still allows reorientation of the mesogens. The change in orientation of the mesogens upon temperature changes or application of an electric field can then produce stresses and strains that are transferred via the polymer to do mechanical work. Note that mechanisms of actuation in LCEs are very similar to the ferroelectrics described above, with the exception that the polarized units do not form part of the polymer backbone itself, but rather are appendages extending from it.

Rate is limited by heat transfer time constants when thermally driven. For a step change in temperature applied to the surface of a thin film of material, an estimate of the time constant of the diffusive heat transfer within the polymer itself can be given as:

$$\tau = R_{th} \cdot C_{th} = \rho \cdot C_v \cdot L^2 \qquad (3)$$

where $R_{th} = \rho \cdot L / A$, $C_{th} = C_v \cdot L \cdot A$, and ρ is the thermal resistivity, C_v is the volumetric heat capacity, A is the area perpendicular to the heat flow, and L is the distance the heat must diffuse. The quantity $(\rho \cdot C_v)^{-1}$ is known as the thermal diffusivity. Leister et al. [23] measured the thermal diffusivity for a ferroelectric liquid crystalline elastomer with a polysiloxane backbone and found values of 2×10^{-8} to 4×10^{-8} m^2/s. For a flat film with a thickness of 100 μm, the corresponding time constant is between 0.25 and 0.5 s. The rate is expected to be proportional to the inverse square of thickness, so it should be possible to activate a 1 μm thick film in less than 100 μs.

Ferroelectric liquid crystals contract and expand when an external electric field is applied to the polymer. The mesogenic units in ferroelectric liquid crystals have an intrinsic polarization. The application of the field changes the alignment of the mesogens and, if they are attached to a polymer backbone, can induce bulk stressses and strains.

Unlike thermal energy, electric fields can be applied through the bulk of the material very quickly, so the response speed is considerably faster in electrostatic-driven films than during thermally induced activation. The time taken to reorient the liquid crystal units is the ultimate rate-limiting factor in ferroelectric liquid crystalline elastomers. In experiments designed to determine the speed to the mesogenic reorientation, Skupin, et al. [27] used time resolved FTIR to measure a response of ~ 10 ms. It should be expected that the response time depends greatly on the specific mesogens used, the polymer backbone structure, and the degree of cross-linking.

In separate experiments by the same group [22], 4% electrostrictive strains were observed in a ferroelectric liquid crystalline elastomer at 133 Hz. In these experiments an electric field of 1.5 MV/m was applied to a thin (75 nm) microtomed sample. Results at other excitation frequencies were not presented and so it is not clear what the frequency dependence of the response looks like.

The low stiffness of these materials means that resonant frequencies will also tend to be low.

Features: Fast response times (~10 ms by field driven actuation [22]), and moderate to large strains. The applied fields (1.5 MV/m) are lower than those used in other ferroelectrics and in dielectric elastomers, leading to correspondingly lower applied voltages for the same thickness of material.

These materials can also be activated via radiative heating, which can potentially create fast activation in one direction providing absorption can be made uniform (cooling will still rely on thermal conduction) [26].

Limitations: Investigation of LCEs is still at a very early stage with the result that much information has yet to be collected. These materials are elastomers with low stiffness and tensile strength so that a relatively small change in load can easily lead to a large change in length. Thermal activation is limited by Carnot efficiency, and heating must continue during activation periods (unless cooling can be turned on and off). The rate of thermal actuation is limited by heat transfer rates. Very fast rates might be achieved using an laser heating, but at the cost of further reduced efficiency.

References:

[17] Brand, H. R. Electromechanical Effects in Cholesteric and Chiral Smectic Liquid-Crystalline Elastomers. Makromolekulare Chemie-Rapid Communications. 1989 Sep; 10(9):441-445.

[18] Finkelmann, H.; Nishikawa E.; Pereira G., and Warner M. A New Opto-Mechanical Effect in Solids. Physical Review Letters. 2001 Jul 2; 87(1).

[19] Kremer, F.; Skupin, H.; Lehmann, W.; Hartmann, L.; Stein, P., and Finkelmann, H. Structure, Mobility, and Piezoelectricity in Ferroelectric Liquid Crystalline Elastomers.; 113 pp. 183-201. (Advances in Chemical Physics.

[20] Lehmann, W.; Hartmann, L.; Kremer, F.; Stein, P.; Finkelmann, H.; Kruth, H., and Diele, S. Direct and Inverse Electromechanical Effect in Ferroelectric Liquid Crystalline Elastomers. Journal of Applied Physics. 1999 Aug 1; 86(3):1647-1652.

[21] Lehmann, W.; Leister, N.; Hartmann, L.; Geschke, D.; Kremer, F.; Stein, P., and Finkelmann, H. Piezoelectric and Pyroelectric Investigations on Microtomized Sections of Single-Crystalline Ferroelectric Liquid Crystalline Elastomers (Sc-Flce). Molecular Crystals and Liquid Crystals Science and Technology Section a-Molecular Crystals and Liquid Crystals. 1999; 328:437-445.

[22] Lehmann, W.; Skupin, H.; Tolksdorf, C.; Gebhard, E.; Zentel, R.; Kruger, P.; Losche, M., and Kremer, F. Giant Lateral Electrostriction in Ferroelectric Liquid- Crystalline Elastomers. Nature. 2001 Mar 22; 410(6827):447-450.

[23] Leister, N.; Lehmann, W.; Weber, U.; Geschke, D.; Kremer, F.; Stein, P., and Finkelmann, H. Measurement of the Pyroelectric Response and of the Thermal Diffusivity of Microtomized Sections of 'single Crystalline' Ferroelectric Liquid Crystalline Elastomers. Liquid Crystals. 2000 Feb; 27(2):289-297.

[24] Meier, W. and Finkelmann, H. Liquid-Crystal Elastomers With Piezoelectric Properties. Mrs Bulletin. 1991 Jan; 16(1):29-31.

[25] Roy, S. S.; Lehmann, W.; Gebhard, E.; Tolksdorf, C.; Zentel, R., and Kremer, F. Inverse Piezoelectric and Electrostrictive Response in Freely Suspended Flc Elastomer Film as Detected by Interferometric Measurements. Molecular Crystals and Liquid Crystals. 2002; 375:253-268.

[26] Shenoy, D. K.; Thomsen, D. L.; Srinivasan, A.; Keller, P., and Ratna, B. R. Carbon Coated Liquid Crystal Elastomer Film for Artificial Muscle Applications. Sensors and Actuators a-Physical. 2002 Feb 28; 96(2-3):184-188.

[27] Skupin, H.; Kremer, F.; Shilov, S. V.; Stein, P., and Finkelmann, H. Time-Resolved Ftir Spectroscopy on Structure and Mobility of Single Crystal Ferroelectric Liquid Crystalline Elastomers. Macromolecules. 1999 Jun 1; 32(11):3746-3752.

[28] Thomsen, D. L.; Keller, P.; Naciri, J.; Pink, R.; Jeon, H.; Shenoy, D., and Ratna, B. R. Liquid Crystal Elastomers With Mechanical Properties of a Muscle. Macromolecules. 2001 Aug 14; 34(17):5868-5875.

[29] Thomsen, D. L.; Keller, P.; Pink, R.; Naciri, J.; Shenoy, D., and Ratna, B. R. Mechanical Responses Approaching Stress, Strain, and Time Scale Properties of Muscle Using Anisotropic Liquid Crystalline Elastomers (Lces). Abstracts of Papers of the American Chemical Society. 2000 Aug 20; 220:272-PMSE.

E. Conducting Polymer Actuators

Synonyms: Conjugated polymers

Mechanisms: Conducting polymers are electronically conducting organic materials. Electrochemically changing oxidation state leads to addition or removal of charge from the

polymer backbone and a flux of ions to balance charge. This ion flux in or out of the material, which can be accompanied by solvent, is associated with swelling or contraction of the material ([30-32]). Insertion of ions between polymer chains appears to be primarily responsible for dimensional changes, although conformational changes of the backbone may also play a role. Changes in dimension may also be chemically triggered [33].

TABLE V
CONDUCTING POLYMER ACTUATORS

PROPERTY	MIN.	TYP.	MAX.	LIMIT	REFS.
Strain (%)		2	30		35,36
Stress (MPa)		5	34	200	30,35,36
Work Density (kJ/m^3)		100			35
Strain Rate (%/s)		1	12		44,45
Power (W/kg)			150		
Life (cycles)		28000	800000		44
Coupling		0.1	1		37
Efficiency (%)		0.1	18	100?	37
Modulus (GPa)	0.2	0.8	3		35,37,41,44
Tensile Strength (MPa)		30	120		37
Applied Potential (V)	0.1	1.2	10		45
Charge Transfer (C/m^3)	1E+07		1E+08		35,37,38
Conductivity (S/m)		10,000	45,000		37
Cost (US$/kg)	3		1000		37

Features: High tensile strength (120 MPa) and stress (up to 34 MPa [34]), Low Voltage (~ 2 V), Catch State (no work performed to maintain fixed load), Stiff (~ 1 GPa modulus [35,36]).

Limitations: The electromechanical coupling in these materials is often less than 1 % [37,38]. As a result, efficiency is also low unless a substantial portion of the input energy is recovered. A consequence of the low electromechanical coupling and the low activation voltages is that very high currents can be required to operate at high power [35], putting constraints on the power supply. Encapsulation issues need to be addressed in order to isolate actuators from the environment. The moderate strains (~2 %) require mechanical amplification in most applications.

Modeling: Experiments show that strain, ε, is proportional to the density of charge, ρ, transferred over a range of strains of about 0.5 %:

$$\varepsilon = \frac{\sigma}{E} + \alpha \cdot \rho \qquad \text{(X)}$$

where σ is the applied stress and E is the elastic modulus [30,32,36-38]. The strain to charge ratio, α, is typically in the range of $\pm 1\text{-}3\times10^{-10}$ m^3·C^{-1} [37]. The sign of the strain to charge ratio is negative when cations dominate the ion transfer and positive when it is anions that serve to balance charge [31]. The ion that dominates is generally the smallest of the available cations and anions. For larger strains this relationship continues to hold to first order. At stresses of more than 5 MPa, effects of creep and stress relaxation begin to become significant, and so the purely elastic model is no longer sufficient [34].

If the strain to charge ratio is re-expressed in terms of change in volume per ion transferred, the volume corresponds approximately to the size of an ion [37]. However, the correlation between ion size and strain to charge ratio is weak [39].

Rate of actuation is primarily limited by the rate at which charge can be injected. Charge transfer is restricted by the internal resistance of the cell and by the rate at which ions are transferred within the polymer [35]. The fastest response is observed in thin films with closely spaced electrodes that employ highly conducting polymer.

Materials and Dimensions: Polypyrrole and polyaniline are the most widely used materials . There has also been some use of polyacetylenes [40], polythiophenes and polyethyldioxithiophene (ref). Monomers are available (e.g. www.aldrich.com, www.basf.com) for all these materials. The most common mode of synthesis is electrodeposition, producing thin (~40 μm thick) films with typical widths of 10 mm and lengths of 1 m or more [37]. They can also be electrodeposited as tubes [41], or chemically synthesized [42]. The properties of the polymers are very dependent on the solvent and salts used in deposition [43], and also the electrolyte employed during actuation [31,36,44]. The life for example can be extended to at to least one million cycles from several tens of thousands by using ionic liquid electrolytes [44].

Forces produced by actuators have reached several Newtons with displacements of several millimeters. Use of mechanical amplification increases displacements up to about 100 mm [45]. Voltages of up to 10 V are used to drive currents that reach several hundred milliamperes. Voltages of only 1-2 V are sufficient for activation, but higher voltages help speed actuation [45]. At steady state (no motion) current is minimal, even when forces are applied.

Temperature: Very little work has been done to characterize the response of conducting polymer actuators under conditions other than room temperature. Changes in the creep behavior between body temperature and room temperature have been reported. Also, the conductivity of the polymer is known to be a function of temperature and synthesis conditions [46,47]. Polymers that exhibit a large temperature dependence of conductivity will be slower at low temperatures due to the increase in internal resistance. Electrolyte conductivity and ion diffusion rates are anticipated to decrease in proportion to the square root of absolute temperature, thereby affecting rates at low temperatures. Finally, solvents and electrolyte freezing will drastically reduce rate. Typical freezing temperatures are between –60°C and 0°C.

Key Investigators and Corporations:

R.H. Baughman, University of Texas at Dallas; Danilo De Rossi & Alberto Mazzoldi, University of Pisa; Ian Hunter, MIT; Keiichi Kaneto, Kyushu Institute of Technology; J. Madden, University of British Columbia; T. Otero; E. Smela, University of Maryland; G. Spinks, G. Wallace and N. Barisci, University of Wollongong; K. West, Technical University of Denmark; www.MicroMuscle.com; www.MolecularMechanisms.com .

Applications: Demonstration braille cells [44] and variable camber blades have been built (www.molecularmechanisms.com). On the micro-scale cell traps,and medical devices are being created (www.Micromuscle.com).

Potential: Layers of thin porous films could enable extremely fast, high power response (> 100 kW/kg). Recovery of stored electrochemical energy should enable moderate efficiencies to be achieved even at full strain (> 10 %). Newly designed conducting polymers promise larger strains and higher electromechanical coupling, but are still at an early stage of development (see next section).

References:

[30] Baughman, R. H., Conducting polymer artificial muscles *Synthetic Metals*, vol. 78, pp. 339-353, Apr 15, 1996.

[31] Pei, Q. and Inganas, O., Electrochemical Application of the bending beam method. 1. Mass transport and volume changes in polypyrrole during redox. *Journal of Physical Chemistry*, vol. 96, pp. 10507-10514, 1992.

[32] Otero, T. F. Artificial Muscles, electrodissolutoin and redox processes in conducting polymers. In: *Handbook of organic and conductive molecules and polymers*, ed. Nalwa, H. S. Chichester: John Wiley & Sons, 1997.pp. 517-594.

[33] Herod, T. E. and Schlenoff, J. B., Doping induced strain in polyaniline: stretchoelectrochemistry *Chemistry of Materials*, vol. 5, pp. 951-955, 1993.

[34] Madden, J. D., Madden, P. G., Anquetil, P. A., and Hunter, I. W., Load and time dependence of displacement in a conducting polymer actuator *Materials Research Society Proceedings*, vol. 698, pp. 137-144, 2002.

[35] Madden, J. D., MaddenPeter G.., and Hunter, I. W. Conducting polymer actuators as engineering materials. In: *Proceeding of SPIE Smart Structures and Materials 2002: Electroactive Polymer Actuators and Devices*, ed. Yoseph Bar-Cohen. Bellingham, WA : SPIE Press, 2002.pp. pp. 176-190.

[36] Mazzoldi, A., Della Santa, A., and De Rossi, D. Conducting polymer actuators: Properties and modeling. In: *Polymer Sensors and Actuators*, eds. Osada, Y. and De Rossi, D. E. Heidelberg: Springer Verlag, 1999.

[37] Madden, J. D. Conducting Polymer Actuators. In: *Ph.D. Thesis*, Anonymous Cambridge, MA: Massachusetts Institute of Technology, 2000.

[38] Madden, J. D., Madden, P. G., and Hunter, I. W. Characterization of polypyrrole actuators: modeling and performance. In: *Proceedings of SPIE 8th Annual Symposium on Smart Structures and Materials: Electroactive Polymer Actuators and Devices*, ed. Yoseph Bar-Cohen. Bellingham WA: SPIE, 2001.pp. 72-83.

[39] Kaneko, M., Fukui, M., Takashima, W., and Kaneto, K., Electrolyte and strain dependences of chemomechanical deformation of polyaniline film *Synthetic Metals*, vol. 84, pp. 795-796, 1997.

[40] Baughman, R. H., Shacklette, R. L., and Elsenbaumer, R. L. Micro electromechanical actuators based on conducting polymers. In: *Topics in Molecular Organization and Engineering, Vol.7: Molecular Electronics*, ed. Lazarev, P. I. Dordrecht: Kluwer, 1991.pp. 267

[41] Ding, J., Liu, L., Spinks, G. M., Zhou, D., Wallace, G. G., and Gillespie, J., High performance conducting polymer actuators utilizing a tubular geometry and helical wire interconnects *Synthetic Metals*, vol. pp. 8In Press.

[42] Kaneto, K., Kaneko, M., Min, Y., and MacDiarmid, A. G., "Artificial muscle" : Electromechanical actuators using polyaniline films *Synthetic Metals*, vol. 71, pp. 2211-2212, 1995.

[43] Yamaura, M., Hagiwara, T., and Iwata, K., Ehancement of electrical conductivity of polypyrrole film by stretching: counter ion effect *Synthetic Metals*, vol. 26, pp. 209-224, 1988.

[44] Wallace, G. , Zhou, D., Ding, J., Xi, B., Innis, P., Mazurkiewicz, J., Spinks, G., Gillespie, J., MacFarlane, D., Forsyth, S., and Forsyth, M., Ionic liquids and helical interconnects: bringing the electronic braille screen closer to reality *Proceedings of SPIE Smart Structures and Materials*, vol. In Press, 2003.

[45] Madden, J. D., Cush, R. A., Kanigan, T. S., and Hunter, I. W., Fast contracting polypyrrole actuators *Synthetic Metals*, vol. 113, pp. 185-193, May, 2000.

[46] Yamaura, M., Hagiwara, T., and Iwata, K., Enhancement of electrical conductivity of polypyrrole film by stretching: counter ion effect *Synthetic Metals*, vol. 26, pp. 209-224, 1988.

[47] Kohlman, R. S. and Epstein, A. J. Insulator-metal transistion and inhomogeneous metallic state in conducting polymers. In: *Handbook of Conducting Polymers*, eds. Skotheim, T. A., Elsenbaumer, R. L., and Reynolds, J. R. New York: Marcel Dekker, 1998.pp. 85-122.

F. Molecular Actuators

Mechanism: Electrochemically or chemically activated single polymers molecules whose molecular structure reversibly changes conformation, leading to mechanical deformations as charge is added or removed. Work is performed from the molecular level up, leading to displacement and performance from the microscopic to macroscopic level. These materials are still at an early stage of development.

Features: Low Voltage (~ 2 V), Large strain (>20 %). Expected to achieve high efficiencies and stresses.

Theory: Molecular conformational changes are induced in materials designed to utilize a variety of molecular mechanisms such as the *cis-trans* photoactivated transition, molecular bending in thianthrene or the π–π molecular dimerization to cite a few (Anquetil, Marsella). In principle, the molecular structure is organized in order to maximize displacement and efficiency.

Example: Poly(calix[4]arene bis-bithiophene)

Poly(calix[4]arene bis-bithiophene) (poly(CalixBBT)), employs hinge molecules (calix[4]arene) interconnected by rigid rods (quarterthiophene). The rods attract one another in the oxidized state, contracting the material into a folded molecular structure. This molecular contraction is driven by the π–π dimerization (π–π stacking) of thiophene oligomers rods upon oxidation, producing a reversible molecular displacement [Kingsborough R.P. and Swager T.M. 1999. The cone conformation of the calix[4]arene scaffold allows generation of an accordion-like molecule upon polymerization under either electrochemical or chemical conditions.

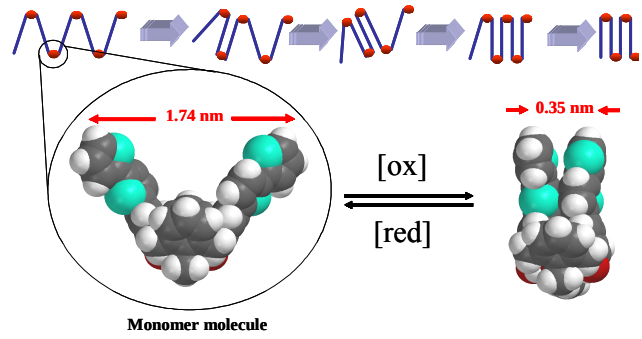

Figure1: Schematic actuation mechanism of poly(CalixBBT).

Poly(calixBBT) is a promising actuating material. Key features of this material include the deformable calix[4]arene scaffold and the redox active quarterthiophene redox units.

The proposed actuation mechanism and a 3-dimensional space-filling model are shown conceptually in Figure 1. The initial polymer displays an equilibrium conformation that has the quarterthiophene groups in a non-aggregated state. Upon oxidation the quarterthiophene groups have a strong tendency to aggregate into a π-stacked structure. Simple inspection of the space-filling model in suggests that one dimensional changes as large of a factor of 9 are possible for Poly(calixBBT)**.**

The proposed molecular actuation mechanism presented above and referred as π-dimerization or π–π stacking makes use of wavefunction overlap in π–conjugated polymers. The π-dimerization is attractive in the oxidized state (electron deficient) and repulsive in the reduced state (filled electronic levels).

It is hoped that these materials will overcome two important deficiencies of conducting polymer actuators, namely the limited strain and the low degree electromechanical coupling, while maintaining the advantage of low voltage operation. To date ~ 20 % strains have been observed in electrochemically activated π-π stacking polymers (Anquetil) and tensile strengths are in the 10's of megapascals.

Limitations. This technology is in an early phase of research. A potential challenge is that the new molecules are unlikely to achieve the same high conductivity as polypyrrole and polyaniline. Low conductivity slows charging and reduces power output. However, conductivity is not as important in these new materials because the number of charges required to achieve displacement is substantially smaller (~100×).

Key Investigators and Corporations:

Hunter I.W., MIT, & Swager T.M., MIT

Marsella M. J., UC Davis

Molecular Mechanisms, LLC,

http://www.molecularmechanisms.com .

[48] Azumi R., Goetz G. and Baeuerle P., Self-Assembly of Alkylsubstituted Oligothiophenes", *Synthetic Metals*, Vol. **101**, pp. 569-572; 1999.

[49] Brocks G., π-dimers of oligothiophene cations", *Journal of Chemical Physics*, Vol. **112**, (12): pp. 5353-5363; 2000.

[50] Graf D.D., Campbell J.P., Miller L.L. and Mann K.R., Single-Crystal X-ray Structure of the Cation Radical of 3',4'-Dibutyl-2,5"-diphenyl-2,2'-terthiophene: Definitive Evidence for π-Stacked Oxidized Oligothiophenes", *Journal of the American Chemical Society*, Vol. **118**, pp. 5480-5481; 1996.

[51] Israelachvili J. Intermolecular and surface forces. 2nd ed, p. 88 ed. London, San Diego: Academic Press; 1991. xxi, 450 p .

[52] Kingsborough R.P. and Swager T.M., Polythiophene Hybrids of Transition-Metal Bis(salicylidenimine)s: Correlation between Structure and Electronic Properties", *Journal of the American Chemical Society*, Vol. **121**, (38): pp. 8825-8834; 1999.

[53] Marsella M.J. and Reid R.J., Toward Molecular Muscles: Design and Synthesis of an Electrically Conducting Poly[cyclooctatetrathiophene]", *Macromolecules*, Vol. **32**, pp. 5982-5984; 1999.

[54] Marzari N. and Schleris Perel D., private communication.

[55] Sirringhaus H., Brown P.J., Friend R.H., Nielsen M.M., Bechgaard K., Langeveld-Voss B.M.W., Spierling A.J.H., Janssen R.A.J., Meijer E.W., Herwing P. and de Leeuw D.M., Two-Dimensional Charge Transport in Self-Organized, High-Mobility Conjugated Polymers", *Nature*, Vol. **401**, pp. 685-689; 1999.

[56] Yamamoto T., Kamarudin D., Arai M., Lee B.-L., Suganuma H., Asakawa N., Inoue Y., Kubota K., Sasaki S., Fukuda T. and Matsuda H., Extensive Studies of π Stacking of Poly(3-alkylthiophene-2,5-diyl)s and Poly(4-alkylthiazole-2,5-diyl)s by Optical Spectroscopy, NMR Analysis, Light Scattering Analysis, and X-ray Crystallography", *Journal of the American Chemical Society*, Vol. **120**, pp. 2047-2058; 1998.

G. Carbon Nanotube Actuators

TABLE VI
CARBON NANOTUBE ACTUATORS [57,58]

PROPERTY	MIN	TYP.	MAX	LIMIT
Strain (%)		0.2	1	1
Stress (MPa)		1		20,000
Work Density (kJ/m^3)		2		2E+08
Strain Rate (%/s)		0.6	19	190000
Power (W/kg)		10	270	1.65E+11
Life (cycles)				
Coupling		0.00067		1.0
Efficiency (%)		0.1	18	1
Density (kg/m^3)		230	1000	2000
Modulus (GPa)	0.2	0.9	30	640
Tensile Strength (MPa)		5		
Applied Potential (V)	0.1	1	30	4
Charge Transfer (C/m^3)		5980000		26,000,000
Conductivity (S/m)		40,000		500,000
Cost (US$/kg)		100000		10

Mechanisms: Carbon nanotubes (CNT) are hollow cylinders consisting solely of carbon. These tubes have diameters that are typically 1.2 nm or larger. Their structure is that of a single rolled sheet of graphite. These sheets are either conductive or semi-conductive. CNT papers and fibers are filtered or spun from large numbers of nanotubes suspended in solution and are actuated by placing them in an electrolyte and activating them using an apparatus very similar to that used for conducing polymers. The application of potential causes the formation of an electrical double layer at the nanotube/electrolyte interface, in which the electronic charge stored in the carbon atoms is balanced by the ionic charge in the liquid phase. The accumulated charge stored in the nanotube is believed to cause a change in the C-C bond length during electron injection [57], producing strains of up to 1 %. Although the strains are small, individual carbon nanotubes are believed to exhibit tensile strengths exceeding 1 GPa, creating an unmatched work per actuator stroke.

As in conducting polymers, it is the rate at which charge can be injected which determines the strain rate. The enormous internal surface area provided by the carbon nanotubes results in an enormous capacitance (26 F/g) [58]. Given the applied potentials are on the order of 1 V, the resulting charge transfer is ~ 26 C/g. Once again the reduction of cell internal resistance is key to achieving high strain rates [59]. Rates of ion transport within the carbon nanotube papers and fibres may also limit rate, although this effect is smaller than in conducting polymers.

Materials & Dimensions: Carbon nanotubes can be synthesized by laser ablation, arc discharge, chemical vapour and deposition from low cost precursors, and are commercially available from many sources. Typical sample dimensions are 30 μm thick, 10 mm wide and 30 mm long films [59].

Limitations: The small to moderate strains require some mechanical amplification for most applications. The electromechanical coupling is poor, requiring substantial energy recovery to achieve reasonable efficiencies. The material cost is currently very high (~$100/g). Films and fibres still exhibit bulk mechanical properties that fall far short of those of single nanotubes. This actuator technology is very new however, and progress on many of these issues is expected to be rapid.

Potential: Individual carbon nanotubes feature very large tensile strength (>10 GPa) and modulus (640 GPa). If these properties can be approached in bulk materials, then the work density per cycle produced will be unmatched (200 MPa). Use of thin films or fibers and closely spaced electrodes should also enable very high strain rates and power to mass ratios to be achieved [35], outperforming piezoceramic materials. Newly reported porous metals appear to be actuated using mechanisms similar to those in CNTs, and could provide high performance relatively soon at lower cost.

Key Investigators and Corporations:

R. . H. Baughman, U. of Texas at Dallas; G. Wallace/G. Spinks/N. Barisci, U. of Wollongong; D. De Rossi & A. Mazzoldi, U. of Pisa; J. Madden, U. of British Columbia; I. Hunter & P. Anquetil, MIT.

References:

[57] Ray H. Baughman, Cui Chanxing, Anvar A. Zakhidov, Zafar Iqbal, Joseph N Barisci, Geoff M. Spinks, Gordon G. Wallace, Alberto Mazzoldi, Danilo De Rossi, Andrew G Rinzler, Oliver Jaschinski, Siegmar Roth, Miklos Kertesz, "Carbon nanotube actuators", Science 284, 1999, pp. 1340-1344.

[58] J.N. Barisci, G.G. Wallace and, G. Spinks, "Electrochemical Characterization of Single-Walled Carbon Nanotube Electrodes." Journal of the electrochemical society 147, 2000, p. 4580.

H. Ionic Polymer/Metal Composites (IPMC)

Overview: An ionic polymer-metal composite (IMPC) consists of a polymeric electrolyte sandwiched between two thin metal layers. Deflection of the layered structure towards one of the metal electrodes occurs as a result of a field induced change in ion concentration, which attracts water molecules to one side of the polymer. The non-uniform distribution of water produces swelling of one side of the actuator and contraction of the other. Unlike other actuator technologies that have been discussed, this technology does not produce linear actuation but only bending.

TABLE VII
IONIC POLYMER METAL COMPOSITES [59]

PROPERTY	MIN.	TYP.	MAX.
Strain (%)			3.3
Stress (MPa)			0.93
Work Density (kJ/m^3)			3
Strain Rate (%/s)			3.3
Power (W/kg)			8.23E-04
Life (cycles)			
Coupling			3
Efficiency (%)			3
Modulus (GPa)	0.1		1.8
Tensile Strength (MPa)			
Density (kg/m3)		2100	
Applied Potential (V)	2		7
Charge Transfer (C/m^3)		900000	
Charge Transfer (C/m^2)		900	
Conductivity (S/m)			
Cost (US$/kg)	500	50000	

Mechanisms: When an electric field is applied across a strip of IPMC, the ions redistribute themselves, resulting in the formation of two thin boundary layers- a cation-poor layer on the anode side of the polymer and a cation-rich layer on the cathode side. The volume change of the boundary layers upon actuation is a result of the volume change of the hydrophilic clusters that are characteristic of the polymer electrolytes used. [59-62] Water diffuses into the cation-rich clusters, which expand due to the increase electrostatic and osmotic pressure. The strain in the cathode layer induces stresses in the rest of the polymer matrix, resulting in bending.[59] Reversing the applied potential inverts the bending.

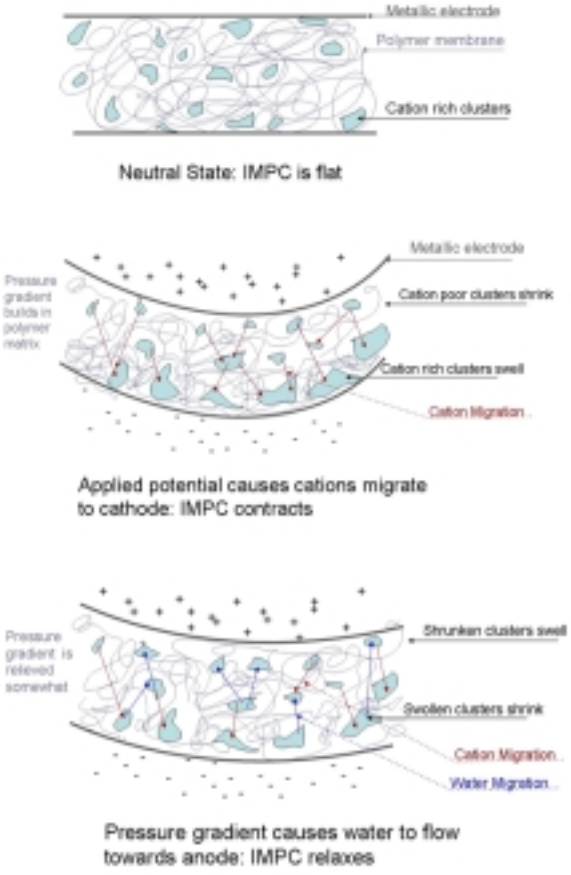

Figure 2: IPMC Actuation.

Materials & Fabrication: Typical polymers are perfluorinated alkenes with anionic-group-terminated side chains, such as Nafion™,[59,60] and Flemion,™ or styrene/divinylbenzene-based polymers with ionic groups substituted from phenyl rings.[59,60] Styrene/divinylbenzene based polymers tend to be highly cross-linked, so their potential as an actuator is severely limited by their stiffness. The perfluorinated alkenes, on the other hand, can arrange

themselves into a flexible orientation.[60] The backbone of the polymer is hydrophobic while the anions used to dope the polymer are hydrophilic. This causes the polymers to make clusters of concentrated anions and neutralizing cations within the polymer network.[60-62]

In most cases, a commercially available polymer membrane is used for the polymer layer. These membranes are not manufactured specifically for IMPCs, however, and limits the IMPCs to a thickness of approximately 200μm.[59] Kim and Shahinpoor have addressed this problem by solution recasting Nafion™ film to a thickness ranging from 30μm to 2mm[59].

Both sides of the polymer membrane are loaded with metal nanoparticles and then metal plated.[60-62] The nanoparticles balance the charging that occurs in the clusters in the boundary layers of the polymer, while the metal plating increases surface conductivity. The metal nanoparticles are usually 3-10 μm in diameter and are distributed in a 10 to 20 μm deep layer both surfaces. This is often done by allowing the polymer to soak in a solution containing a metal salt, such as $Pt(NH_3)_4HCl$, so the metal ions can diffuse into the polymer. The polymer is then treated with a reducing agent, such as $LiBH_4$ or $NaBH_4$, to metalize the polymer. The primary reaction for platinum IMPCs is as follows: [60,62]

$$LiBH_4 + 4[Pt(NH_3)_4]^{2+} + 8OH^- \Rightarrow 4Pt^o + 16NH_3 + LiBO_2 + 6H_20 \quad (2)$$

To reduce this cost, Shahinpoor and Kim physically load the metal particles into the polymer. [60] The polymer and metal powder can be composited by pressing under high pressure and temperature (Shahinpoor and Kim pressed under 2 tons at 130°C for 15 minutes, 3 times). The electrode layer can then be deposited onto the surfaces. IMPCs manufactured in this way have shown comparable properties to chemically loaded IMPCs, at 1/10 of the manufacturing cost. [60]

The plating is usually 1 to 5 μm thick.[60] It again involves reduction of a metal salt. However, instead of impregnating the metal into the polymer, the reaction coats the surface of the composite. Metals that have been successfully used for this process include platinum, palladium, silver, gold, carbon, graphite, carbon nanotubes [60,62] as well as copper.[62] Platinum is the most commonly used as it is has the widest potential region over which it is resistant to corrosion. The higher potential enables larger deflection and higher work density. The electrode reduces the surface-electrode resistance down to as little as 8.6% of its original value[62].

Key Investigators and Corporations:

Moshen Shahinpor, University of New Mexico.
Yoseph Bar-Cohen, NASA Jet Propulsion Lab.
Biomimetic Products Inc. http://www.biomimetic.com/

[59] Kim, K.J., Shahinpoor, M. *Polymer* 43 (2002) 797-802
[60] Shahinpoor, M. Kim, K.J. *Sensors and Actuators A* 96 (2002) 125-132
[61] Shahinpoor, M., Kim, K.J. *Smart Mater. Struct.* 10 (2001) 819-833
[62] Shahinpoor, M., Kim, K.J. *Smart Mater. Struct.* 9 (2000) 543-551

I. Magnetostrictives

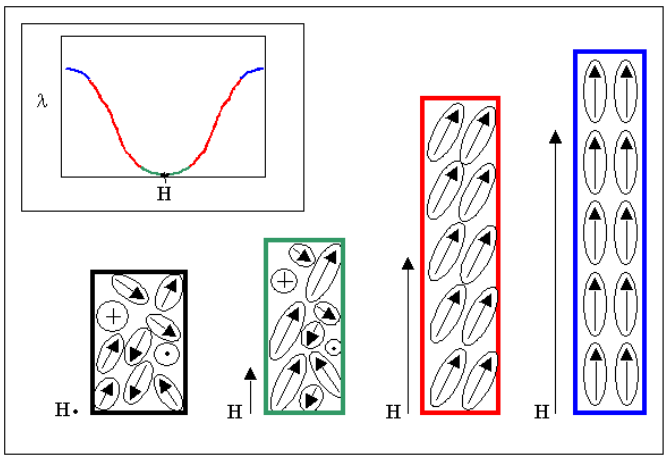

Figure 3: Magneto-striction.

History: Over a century after Joule's discovery of the conversion of magnetic energy to mechanical energy, the magnetostrictive effect again sparked scientific interest upon the discovery of giant magnetostriction in Lanthanide metals. Arthur Clark, in his early review of the subject [63], presents a detailed account of the investigations and insight that prompted the development of rare earth alloys capable of strains on the order of 1.0 x 10^{-3} at room temperature. This represented an increase of two orders of magnitude over magnetostrictive strains observed by Joule and obtainable in common transition metals such as Fe, Co, and Ni. By 1974, it was postulated that the alloy $Tb_{0.3}Dy_{0.7}Fe_2$ would exhibit large magnetostriction with a relatively small applied field at room temperature [64]. Indeed, nearly thirty years later, a commercially available product of the same nominal composition, known as Terfenol-D, is capable of producing strains of 1.6 x 10^{-3} with an applied field of 2.0 MA/m and power densities of 10-20 kJ/m^3 [65].

Mechanism: The process of magnetostriction makes use of the magnetic domains that form within a ferromagnetic material when cooled below its Curie Temperature (*Tc*). The presence of an external magnetic field first grows the domains aligned with the field and then overcomes the anisotropic energy to rotate the magnetic moments of the unaligned domains to a more favorable, easy axis in the crystal. The growth and rotations are accompanied by strains in the bulk material. Strengthening the field further aligns all of the domains completely with the field and leads to saturation. A schematic diagram of the magnetostrictive mechanism is presented in Figure 3 with a representative curve for strain versus applied magnetic field and coinciding with descriptions in the literature [66,67]. The performance of a magnetostrictive material can be well characterized by Curie Temperature *Tc*, saturation magnetostriction λs, and magnetic anisotropy energy *K*. Indeed it was an understanding of these properties that led to the development of Terfenol D [63] which combines a Tc of 380 °C, a λs of 1.6 x 10^{-3} and a K near zero. $TbFe_2$ and $DyFe_2$ have K values of opposite signs, making the minimization possible through variations in composition. Further work has demonstrated that

magnetostrictive materials can be tailored for specific temperature regimes guided by the same principles [68].

Features: For room temperature applications, Terfenol-D is the highest performing magnetostrictive material. It is most commonly utilized in cylindrical forms and driven with solenoids. It has a modulus of 25-30 GPa with tensile and compressive strengths of 28 and 700 MPa respectively [69]. The material properties continue to be improved through numerous methods including single crystal growth, defect study and elimination, and crystal orientation [70], leading to strains of 2.4 x 10^{-3} [71]. Meanwhile, engineering applications have improved the performance of Terfenol-D by applying a bias field with permanent magnets to enable controlled positive and negative deflection and applying a prestress to the material, enabling larger strains by compressing the magnetic domains before the application of a magnetic field. In addition, careful use of device resonance has enabled the observations of dynamic strains of 3.5 x10^{-3} and approximately 50% of electrical energy being converted to work [72]. Cycle lives in the tens of millions have been suggested [65].

TABLE VIII
MAGNETOSTRICTIVE MATERIALS [WWW.EXTREMA.COM]

PROPERTY	MIN.	TYP.	MAX.
Strain (%)		0.1	0.24
Stress (MPa)		20	28
Work Density (kJ/m^3)		20 20	
Strain Rate (%/s)		(10 kHz)	
Power (W/kg)			
Life (cycles)			1o^7
Coupling		0.75	
Efficiency (%)			
Density (kg/m^3)		9210	
Modulus (GPa)	25		35
Tensile Strength (MPa)		28	
Compressive Strength		700	
Applied field (MA/m)		2	

Limitations: The relatively small strains (0.1 to 0.25 %) observed in these materials mean that substantial mechanical amplification is required for many applications. These materials are brittle in tension, failing at stresses of 28 MPa. Magnetostrictive composites have enabled reductions in brittleness while maintaining large strains and increasing bandwidth [73]. Terfenol-D can operate in the frequency range of kHz, though its high conductivity leads to significant eddy currents at higher frequencies. Commercially, laminations of multiple crystals are used to minimize the eddy currents and extend the frequency range. Costs of Terfenol-D depend largely on the availability of the rare earth metals, though costs of high performance composites and single crystals are not yet available.

Temperature: All magnetostrictive materials reversibly lose functionality above *Tc*, while temperatures above the melting point require reprocessing. There are no known material failure mechanisms comparable to depoling of piezoelectric transducers.

Modeling: In his first review, Clark discussed the effects of the magnetic field on the crystallographic planes of cubic and hexagonal lattices, which led to an abundance of characterization constants [63]. Since then, some authors have sought simplified device specific models [72], while others have developed theories based on free energy minimization [67]. Recently, Jiles has focused on the hysteretic effects of magnetoelasticity, a source of considerable difficulty in modeling for practical applications [74]. In his earlier review, however, Jiles gives an excellent description of the development of key parameters to be used in successful application of Terfenol-D [70]. While modeling represents the newest challenge for magnetostrictive materials, it's success has led to many innovations in materials and processing.

Key Investigators:

A. E. Clark, D. C. Jiles (see references below).

Etrema Products Inc (sells actuators and bulk materials www.etrema-usa.com).

References:

[63] A. E. Clark, *Ferromagnetic Materials* vol 1, ed E P Wohlfarth (North-Holland, Amsterdam, 1980) p. 531.

[64] A. E. Clark, *AIP Conf. Proc. 18* (American Institute of Physics, New York, 1974) p. 1015.

[65] http://www.etrema-usa.com.

[66] D. C. Jiles, *Introduction to Magnetism and Magnetic Materials* (Chapman and Hall, New York, 1991).

[67] R. C. Smith, M. J. Dapino, S. Seelecke, J. Appl. Phys. **93**, 458 (2003).

[68] A. E. Clark, *MRS Symp. Proc. 360* (Materials Research Society, Pennsylvania, 1994) p. 171.

[69] H. Janocha, Sensors and Actuators A **91**, 126 (2001).

[70] D. C. Jiles, J. Phys. D: Appl. Phys. **27** 1 (1994).

[71] X. Zhao, G. Wu, J. Wang, K. Jia, W. Zhan, J. Appl. Phys. **79** 6225 (1996).

[72] F. Claeyssen, N. Lhermet, R. Le Letty, P. Bouchilloux, J. Alloys and Compounds **258**, 61 (1997).

[73] L. Sandlund, M. Fahlander, T. Cedell, A.E. Clark, J. B. Restroff, M. Wun-Fogle, J. Appl. Phys. **75** 5656 (1994).

[74] M. J. Sablik and D. C. Jiles, IEEE Transactions on Magnetics **29**, 2113 (1993).

J. Thermally Activated Shape Memory Alloys

History: Over a century after Joule's discovery of the equivalence of energy and heat the shape memory effect was reported by Chang and Reading (1951). They observed that an alloy of gold and copper returns to the same shape if heated after deformation. The same effect was later discovered in Indium-Titanium alloys by Basinski and Christian (1954), and Nickel-Titanium alloys by Buehler, Gilfrich and Wiley (1963). These researchers used the term "Shape Memory Effect" (SMA) to describe the phenomena. Of all the SMA's Nickel Titanium (NiTi) alloys (better known as Nitinol) were the most extensively studied (Funakubo, 1987). NiTi fibers and springs have often been studied and used as artificial muscles (Hashimoto et al., 1985; Bergamasco et al., 1989; Hirose et al., 1985; Homma et al., 1989; Ikuta, 1990; Hunter et al., 1990, 1991) because of their relative nontoxicity, reasonable cost and an electrical resistivity that easily lends itself to Joule heating (passing of an electrical current to generate heat).

TABLE IX
THERMAL SHAPE MEMORY ALLOYS [92]

PROPERTY	MIN.	TYP.	MAX.
Strain (%)		5	8
Stress (MPa)			200

Work Density (kJ/m^3)		>1000	
Strain Rate (%/s)		300	
Power (W/kg)		1000	> 50,000
Life (cycles)	10	10000	10^7
Coupling			
Efficiency (%)		3	5
Modulus (GPa)	20		83
Tensile Strength (MPa)		1000	
Density (kg/m^3)		6450	
Applied Potential (V)	4		1kV/m
Charge Transfer (C/m^2)			
Conductivity (S/m)		1250	1425
Cost (US$/kg)		300	

Mechanism: Martensitic transformations are at the heart of the shape memory effect as shown by Otsuka and Shimizu (1970). Martensitic transformations were discovered by the metallurgist Adolf Martens in steels (Van Humbeeck et al., 1991). It was found that the transformation from the high-temperature, body-centered cubic lattice austenitic phase to the low temperature, face-centered tetragonal lattice takes place without atomic diffusion. Martensitic transformations are phase changes that occur as a displacitive, lattice-distortive, first order diffusionless athermal transformations. In NiTi alloys with a surplus of nickel or with nickel partly replaced with a third element, a two stage martensitic transformation may occur. The intermediate phase has a rhombohedral crystal structure.

In most NiTi alloys the shape memory effect is only observed when an external stress is applied. In the martensitic phase the alloy has a twinned martensite that can be easily deformed as it de-twins. As it is heated it returns to its parent austenic phase which is a highly ordered state the alloys retrieves a well defined high-temperature shape.

NiTi alloys may also exhibit a two-way shape memory effect (TWSM) first observed by Delaey et al. in 1975 and by which the alloy will exhibit the shape memory effect without an external stress. In the two-way shape memory effect NiTi alloys also have a "remembered" state at low temperature as well as all the intermediate shapes between the high temperature and low temperature. The origin of TWSM is stress-biased martensite and it can only be obtained by special conditioning involving thermo-mechanical treatment.

The contraction time of NiTi is governed by the speed at which the martensitic to austenitic phase transformation occurs and hence by the electrical power when electrical Joule heating is used. By using very large current pulses this contraction time can be reduced to several milliseconds (Hunter et al., 1991). The NiTi contraction and expansion cycles are mainly limited by the long time required for NiTi to cool and return to its lower temperature shape. The cooling time is governed by thermal diffusion and convection. Factors such as heat capacity and latent heat involved in the phase transformation between the austenitic and martensitic phases must be considered when designing an actuator.

Features: Shape memory alloys can exert very large forces per unit area (exceeding 200MPa), operate at very high strain rates (300%/s) and undergo relatively large deformations (> 5% for poly-crystalline NiTi fibers). The peak energy density (10^7 J·m^{-3}) and power per unit mass (50 kW·kg^{-1}) of these actuators is unmatched.

Limitations: They however have several characteristics that impede their use as muscle-like actuators. One of them is the difficulty to control the length of NiTi fibers as they undergo a phase transformation. The change in length is observed over a narrow temperature range and a significant hysteresis is observed between the martensitic to austenitic and austenitic to martensitic phases. The phase transformation temperatures vary more or less linearly with stress and the cycling characteristics also change if only partial transformations occur. All of these factors must be modeled appropriately when NiTi fibers are used in a servo-actuator.

NiTi actuators also have a limited lifetime in terms of useable cycles. At very large strains their shape memory effect degrades significantly, from millions of cycles at 0.5% strains to a few hundred cycles at strains of 5% (Funakubo, 1987) depending on the alloy and conditioning. Their usage is also limited by the low efficiency of NiTi fibers in converting electrical energy to mechanical work which is typically found to be limited to less than 5% (including recovery of energy from heat, McCormick 1987).

Materials: Nickel titanium shape memory alloys are commercially available from several sources including Shape Memory Applications Inc. http://www.sma-inc.com/.

Applications: NiTi wires, tubes and components are widely used in medical applications due to their super-elasticity, a property related to the memory effect. Little use is made of the actuation properties.

[75] Basinski, Z.S. and Christian, T. Acta Metallurgica, 1954, 2, 101.

[76] Bergamasco, M. Salsedo, F. and Dario, P. A linear SMA motor as direct-drive robotic actuator. 1989 IEEE International Conference on Robotics and Automation, May, 1989, Scottsdale, Arizona, 618-623.

[77] Bergamasco, M. Salsedo, F. and Dario, P. Shape memory alloy micro-motors for direct-drive activation of dexterous artificial hands. Sensors and Actuators, 1989, 17, 115-119.

[78] Buehler, W.J., Gilfrich, J. and Wiley, K. Journal of Applied Physics, 1963, 34, 1465.

[79] Chang, L.C. and Read, T.A. Transactions of the American Institute of Mechanical Engineers, 1951, 189, 47.

[80] Delaey, L., Thienel, J. Shape Memory Effects in Alloys, Jeff Perkins (Ed), Plenum, 1975, New York, 341-350.

[81] Funakubo, H. (ed.) Shape Memory Alloys. Gordon and Breach: New York, 1987.

[82] Hirose, S., Ikuta, K. and Umetani, Y. A new design method of servo-actuators based on the shape memory effect, in Theory and Practice of Robots and Manipulators, Proceedings of RoManSy'84, the 5th CISM-IFToMM Symposium, Hermes Publishing, 1985, 339-349.

[83] Hirose S., Ikuta, K. and Sato, K. Development of a shape memory alloy actuator. Improvement of output performance by the introduction of a s-mechanism. Advanced Robotics, 1989, 3, 89-108.

[84] Homma, D., Miwa, Y. and Iguchi, N. Micro robots and micro mechanisms using shape memory alloy. The 3rd Toyota Conference Integrated Micro Motion Systems: Micromachining, Control and Application. Nissin, Aichi, Japan, October, 1989, 22, 1-21.

[85] Hunter, I.W. Novel Actuators For Use in Robotics And Tele-Robotics, Report Prepared for the US Office of Naval Research, 1990, 88p.

[86] Hunter, I.W., Lafontaine, S. and Hollerbach, J.M. Artificial muscle prototype for use in robotic and prosthetic limbs. Proceedings of the 16th Canadian Medical and Biological Engineering Conference, 1990, 16, 35-36.

[87] Hunter, I.W., Lafontaine, S., Hollerbach, J.M. and Hunter, P.J. Fast reversible NiTi fibers for use in microrobotics. Proceedings IEEE Micro Electro Mechanical Systems, 1991, 2, 166-170.
[88] Ikuta, K. Micro/miniature shape memory alloy actuator. Proceedings IEEE Micro Electro Mechanical Systems, 1990, 3, 2156-2161.
[89] McCormick, P.G., On the practical efficiency of shape memory engines, Scipta Metallugica 1987 21, 99-101.
[90] Otsuka, K. and Shimizu, K. Scripta Metallurgica, 1970, 4, 469.
[91] Van Humbeeck, J., Chandrasekaran, M. and Delaey, L. Shape memory alloys: materials in action. Endeavour, New Series, 1991a, 15(4), 147-154.
[92] I. Hunter & S. Lafontaine, "A comparison of muscle with artificial actuators", *Technical Digest IEEE Solid State Sensors & Actuators Workshop*, 1992, pp. 178-185.

K. Ferromagnetic Shape Memory Alloys

Synonyms: FSMA

Overview: FSMAs utilize crystallographic transformations to macroscopically change dimension under the influence of a magnetic field. Following the discovery of the thermally induced martensitic transformation in the ferromagnetic Ni_2MnGa Heusler alloy in 1995 [93], it was postulated that large strains could also be obtained magnetically. Scarcely a year later, strains of 0.2% were observed in a single crystal of the same composition upon the rotation of a magnetic (H) field of order 600 kA/m [94]. Further investigation into the effects of varying the atomic composition of the alloy on the martensitic transition and Curie temperatures [95] along with better characterization techniques have since led to measurements of 6% [96] and even 10%[97] linear strain under applied fields of the same order of magnitude. These strains may be obtained against stresses of order 1 MPa and with response times in milliseconds at room temperature.

TABLE X
FERROMAGNETIC SHAPE MEMORY ALLOYS

PROPERTY	MIN.	TYP.	MAX.
Strain (%)			9.5
Stress (MPa)	0.005	1	4
Work Density (kJ/m^3)		95	
Strain Rate (%/s)		2000 (10% @ 100Hz)	
Power (W/kg)			
Life (cycles)			
Coupling		0.75	
Cost (US$/kg)		4400	

Mechanism:
The mechanism encompasses transitions from the cubic austenite phase to the tetragonal martensite phase as well as transitions between variants of the martensite phase. The martensite phase is magnetically easy along its shortest (c) axis and may be aligned mechanically or magnetically. Typically, samples are prestressed in compression to align the anisotropic unit cells. Upon the application of a magnetic field orthogonal to the direction of stress, regions of the magnetically favored variant nucleate and grow. These regions may be monitored by the appearance of twin boundaries, which are observed to move along the sample as the intensity of the field is increased [98,99]. The magnitude of the bias or prestress is important as an insufficient stress will leave the sample uncompressed and an overstress will block the transition. Blocking stresses between 2.0 and 9 MPa have been reported [96,100]. Following the removal of the field, stresses above 0.5 MPa are sufficient to return the sample to original dimensions [66].

Modeling:
O'Handley et al recently reviewed the models currently used in predicting strain vs. magnetic field for FSMAs [101].

Materials:
Single crystal Ni_2MnGa and slight variations.
Other ferromagnetic alloys (such as Fe-Pd and Fe-Ni-Co-Ti) show similar effect, but lower strains.
Polycrystalline Ni_2MnGa also exhibits FSMA behavior, but at reduced strains due to alignment and loading within a matrix [102].

Features:
Large strains (~10%) for a stiff (up to 90 GPa modulus) crystalline alloy system. Fast response (~ 1kHz) and high cycle life (~5×10^7 cycles) [103]. Catch state at low stresses (0.5 MPa).

Limitations:
Requires high intensity magnetic fields (~500 kA/m) and the fields need to be applied orthogonal to stroke direction adding challenge to the device design. Although the stresses against which the actuators will work are relatively large (up to 1 MPa), this does not account for the space needed to generate the required magnetic fields. For example, in Adaptamat Ltd. products the active material produces 1 MPa stresses, but once the coils necessary to produce field are added, the effective stress drops to < 20 kPa [103]; The presence of the coils also drops the work density to 0.12 kJ·m^{-3}. Unidirectional actuation requires a compressive restoring force; Modulus appears to change tremendously between the Austenite and Martensite phases (dropping to 0.02 GPa in the Martensite phase [105]). The compliance may result in low resonance frequencies.

Temperature: Requires operation near the martensitic transformation temperature (200- 350 K) and below Curie temperature (325-350 K), both of which vary with composition [94].

Key Investigators and Corporations: R C O'Handley; K Ullakko; V V Kokorin; A N Vasil'ev; R D James; M Wuttig
Adaptamat Ltd. (www.adaptamat.com)

Applications: Linear motors available from Adaptamat Ltd. operating with strains ~3% at 2 MPa. Raw materials and custom motors also available from same.

Potential: Achieved strain has reached known theoretical limit. However, new passive shape memory effect discoveries may lead to higher strains [104].

References:

[93] V. A. Chernenko, E. Cesari, V. V. Kokorin, I. N. Vitenko. "The Development of New Ferromagnetic Shape Memory Alloys in Ni-Mn-Ga System." *Scripta Metallurgica et Materialis* **33,** pp. 1239-1244 (1995).

[94] K. Ullakko, J. K. Huang, C. Kantner, R. C. O'Handley, V. V. Kokorin. "Large magnetic-field-induced strains in Ni_2MnGa single crystals." *Appl. Phys. Lett.* **69**, pp. 1966-1968 (1996).
[95] A. N. Vasil'ev, A. D. Bozhko, V. V. Khovailo, I. E. Dikshtein, V. G. Shavrov, V. D. Buchelnikov, M. Matsumoto, S. Suzuki, T. Takagi, J. Tani. "Structural and magnetic phase transitions in shape-memory alloys $Ni_{2+x}Mn_{1-x}Ga$." *Phys. Rev. B* **59**, pp. 1113-1120 (1999).
[96] S. J. Murray, M. Marioni, S. M. Allen, R. C. O'Handley, T. A. Lograsso. "6% magnetic-field-induced strain by twin-boundary motion in ferromagnetic Ni-Mn-Ga." *Appl. Phys. Lett.* **77**, pp.886-888 (2000).
[97] A. Sozinov, A. A. Likhachev, N. Lanska, K. Ullakko. "Giant magnetic-field-induced strain in NiMnGa seven-layered martensitic phase." *Appl. Phys. Lett.* **80** pp.1746-1748 (2002).
[98] S. J. Murray, M. A. Marioni, A. M. Kukla, J. Robinson, R. C. O'Handley, S. M. Allen. "Large field induced strain in single crystalline Ni-Mn-Ga ferromagnetic shape memory alloy." *J. Appl. Phys.* **87**, pp. 5774-5776 (2000).
[99] R. Tickle, R. D. James, T. Shield, M. Wuttig, V. V. Kokorin. "Ferromagnetic Shape Memory in the NiMnGa System." *IEEE Trans. Magnet.* **35**, pp.4301-4310 (1999).
[100] R. Tickle, R. D. James. "Magnetic and magnetomechanical properties of Ni_2MnGa." *J. Magn. Magn. Mater.* **195**, pp.627-638 (1999).
[101] R. C. O'Handley, S. J. Murray, M. Marioni, H. Nembach, S. M. Allen. "Phenomenology of giant magnetic-field-induced strain in ferromagnetic shape-memory materials" *J. Appl. Phys.* **87**, pp.4712-4717 (2000).
[102] M. A. Marioni, R. C. O'Handley, S. M. Allen. "Analytical model for field-induced strain in ferromagnetic shape-memory alloy polycrystals." *J. Appl. Phys.* **91**, pp.7807-7809 (2002).
[103] www.adaptamat.com
[104] C. Jiang, T. Liang, H. Xu, M. Zhang, G. Wu. "Superhigh strains by variant reorientation in the nonmodulated ferromagnetic NiMnGa alloys." *Appl. Phys. Lett.* **81**, pp.2818-2820 (2002).
[105] S. Murray, Report to Darpa by Mide Corporation, "Ferromagnetic Shape Memory Alloys: Device Applications", http://www.darpa.mil/dso/thrust/matdev/chap/briefings/timchap2000day3/murray_mide.pdf, 2000.

III. Case Studies

Two case studies that represent promising applications of artificial muscle technology are presented. Both applications are targeted at autonomous underwater vehicles (AUV), where size, power consumption and cost need to be minimized. In the first case, varying propeller blade camber using artificial muscle is proposed. In the second, amplification of propeller thrust by the generation of unsteady flow is presented. In the first application rates are relatively slow – the challenge is to incorporate the actuator within the space allotted. In the second, power to mass and fuel efficiency become critical.

A. Case Study: Variable camber propeller

Controllable pitch propellers are employed in situations where vessels operate under a range of flow conditions. The complex gearing mechanisms employed are too costly to consider in most AUV's. Nevertheless AUVs could benefit tremendously from the added efficiency, maneuverability, and the potentially lower noise emissions afforded by variable shape propellers.

The target vehicle for variable camber is EMATT (Expendable, Mobile ASW Training Target from Sippecan Inc, in Marion, Massachusetts). The expendable nature of the vehicle makes cost a key consideration.

Specifications:

This design is for a propeller blade that has a span (length) of 50 mm, a chord (width) of 25 mm, and a thickness of 6 mm over a 10 mm long pivoting trailing edge and greater than 6 mm over the entire chord, as depicted in Figure 4. The last 10 mm of the chord at the trailing edge are pivoted so as to have variable camber. The angle of the trailing edge is to be adjusted by 45° under a force load of up to 3.5 N.

In order to simplify the calculations the unknown distribution of the force is applied at a single point at 3 mm from the trailing edge. The force of 3.5 N generates a torque of 25 mN·m about the pivot. If the angle of deflection is 45°, the work that must be done is $W = T\,\theta = (25\text{ mN m})\times(\pi/4) =$ 19 mJ. A DC electrical power source capable of delivering up to 9 A at 45 V is available at the propeller. The vehicle lifetime is up to ten hours, over which time up to 10,000 actuation cycles will be performed.

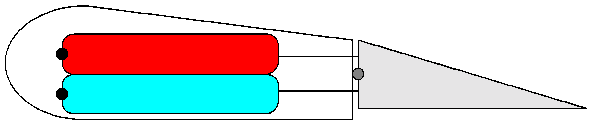

Figure 4: Lever arm design for creating variable camber.

Will the actuator fit within the space?

Ideally the mechanism employed will fit within a propeller blade. The non-pivoting portion of each blade has a volume of $6\text{ mm} \times 15\text{ mm} \times 50\text{ mm} = 4.5 \times 10^{-6}\text{ m}^3$. Given the required work, the minimum work density in order to fit the actuator within the propeller volume is $4.2\text{ kJ}\cdot\text{m}^{-3}$. The higher the work density of an actuator material is above this value, the lower the volume that will be required and the easier will be the fit.

TABLE XI
COMPARISON OF WORK DENSITIES

MATERIAL	WORKDENSITY (KJ/M3)
Skeletal Muscle	0.8
FSMA including coils	<1
Dielectric Elastomer (Silicone)	1.6
Carbon Nanotubes	2
IPMC	3
Magnetostrictive	20
Liquid Crystal Elastomer	56
Dielectric Elastomer (VHB)	58
Ferromagnetic SMA	95
Conducting Polymer	100
Ferroelectric Polymers	320

Thermal SMA	1000

The data in Table XI suggests that skeletal muscle, silicone dielectric elastomers, carbon nanotubes and IPMCs do not currently demonstrate sufficient work density for this application. Inclusion of activation coils needed to generate magnetic field in the energy density calculation eliminates the FSMA (and the magnetostrictives, which require still higher fields). Note that the lower energy densities of these technologies can be compensated for by using multiple actuator strokes to deflect the trailing edge (e.g. using a ratchet mechanism). However, this adds to the complexity and cost of the device.

Mechanical Amplification

The linear actuators discussed range in strain from less than 1% to more than 100%, and the stresses from the low kPa range up to 200 MPa. If the force divided by the cross-sectional area (3.5 N/(50 mm×6 mm)=12 kPa) is less than the stress that an actuator is capable of generating, then no amplification of the force is required. Furthermore, if the strain multiplied by the length of the actuator is roughly equal to the required displacement of the trailing edge (=3 mm×sin(45°)/15mm= 14 % strain), then little or no amplification of the strain is required, simplifying design and fabrication. The ideal actuator will feature both high strain and high stress. Low values of either indicate a need for mechanical amplification, and the smaller the values the greater the amplification. For example, the small strains characteristic of magnetostrictive materials need to be amplified by a factor of ~100. This degree of amplification is unrealistic without resorting to a stepping or ratcheting motion.

Example – LCE Acutation

To make these considerations more concrete, consider designing an LCE actuator for this application. The best performance of a liquid crystal elastomer reported in the literature (Thomsen et al., 2000) has a work density of $\sigma\times\varepsilon$ = (140 kPa)×(0.40) = 56 J/m^3, well over the required work density.

As a simple design exercise, we can model a simple lever arm that pulls around the pivot (see Figure). If the muscle attachment points are a distance of 1 mm from the pivot (in the vertical direction), the muscles must exert a force *F* to balance the torques:

$$F = \frac{(3.5N)(7mm)}{(2mm)} = 12.5N\,.$$ balance of torques

The liquid crystal elastomer can exert a stress of 140 kPa and undergo a strain of up to 40%. The cross-sectional area needed to generate a force of 12.5 N is:

$$A = \frac{12.5N}{140kPa} = 90\times10^{-6}\,m^2$$,cross sectional area for required force

or, if the width of the muscle is taken to be the length of the blade (50 mm), the thickness *h* of the muscle must be:

$$h = \frac{A}{L} = 1.8mm$$ thickness of muscle within the blade

The muscle length that is needed to get a 45° rotation of the trailing edge is roughly $\Delta x = 2\ mm \times \sin(45°) = 1.4\ mm$. If the total strain of the actuator is 40%, then an actuator length of only 3.5 *mm* is needed to give the required deflection. The calculations show that an LCE actuator could be used for this application based on these considerations alone.

Rate

In changing camber, a 1 s response time is ample. All the actuators presented can reach this target. However, in conducting polymers the actuator material thickness cannot exceed ~ 30 μm if the actuator is to respond sufficiently quickly – otherwise diffusion of ions into the polymer will be too slow. A laminated or porous structure is required. Thermally activated liquid crystal elastomers, in which heat must be transferred to or from the polymer, will also need to be laminated into similarly thick layers, and have a mechanism for transferring heat to each layer.

Voltage Requirements

Ferroelectric polymers, dielectric elastomers and, to a lesser degree, liquid crystal elastomers all require high fields in order to produce substantial displacement. In order to prevent voltages from being excessive, these materials will need to be layered. 100 μm thick layers require 1.5 kV in ferroelectric polymers and dielectric elastomers, and 150 V in liquid crystal elastomers (LCE). For optimum performance, these layers should also be pre-strained, further adding to complexity of assembly. Note that for the ferroelectrics and dielectric elastomers in particular, additional cost and space will be needed for DC-DC power converters.

Catch state

In varying camber it is anticipated that one angle of deflection may prove optimal over long periods of time. Thus it best if no power input is required to maintain the desired position. Thermally activated SMAs and LCEs generally require continued heat input in order to hold a fixed position, and thus consume substantial power even when no work is being performed. IPMCs are often characterized by substantial leakage current to maintain fixed position, and in some cases cannot hold a position for more than several seconds. As a result, SMAs and LCEs are not suited for steady state applications (unless steady state is generally in the off position).

Continuously variable positioning

SMAs and LCEs involve phase changes. It is easy to run these phase changes to completion each time actuation is performed, but is a very difficult challenge to control the phases such that an intermediate state is reliably reached. For this reason SMAs and LCEs are not appropriate for the variable camber application.

Having considered energy density, mechanical amplification, voltage, controllability, and energy expenditure, each actuator technology may be accepted or rejected, as presented in Table XII.

TABLE XII
ACTUATOR SELECTION: VARIABLE CAMBER

MATERIAL	ACCEPT?	POTENTIAL PROBLEMS
Skeletal Muscle	No	Work density too low.

Ferromagnetic SMA	No	Coil volume prohibitive.
Dielectric Elastomer (Silicone)	No	Work density too low.
Carbon Nanotubes	No	Work density too low.
IPMC	No	Work density too low.
Magnetostrictive	No	Coil volume prohibitive.
Liquid Crystal Elastomer	o.k.	Control & lamination?
Dielectric Elastomer (VHB)	o.k.	Stiffness & high voltage.
Conducting Polymer	o.k.	Lamination.
Ferroelectric Polymers	o.k.	High voltage.
Thermal SMA	No	Control, no catch state.

There are four candidate actuator technologies that are likely suitable for the variable camber application.

B. *Case Study 2: Unsteady Flow Hydrodynamics*

The work of Hover et. al. in this proceedings demonstrates that adding flapping and rolling motions in a critical range of frequencies to foils and propellers can quadruple thrust for a given propeller rotation rate. Can the artificial muscle technologies meet the demands of this high power application?

The REMUS AUV (http://www.hydroidinc.com/) is chosen as an example platform for application of novel propulsion concepts. REMUS has been selected by the Navy for performing Very Shallow Water Mine Counter Measures (VSW-MCM).

Rate

The REMUS propeller runs at ~ 25 Hz. To create optimum unsteady flow conditions, the blades must then flap at ~ 50 Hz. This bandwidth requirement immediately eliminates thermally activated LCEs, and conducting polymers as candidate materials. As discussed above, it should be possible to drive these materials up to kilohertz frequencies, but current demonstrations operate at ~ 1Hz.

Cycle Life

A REMUS mission lasts up to 22 hours, which corresponds to ~ 2 million actuator cycles. This cycle number is approaching or exceeding the limits so far measured for most technologies. In order to achieve this cycle number, the amplitude of actuation will need to be reduced to ~ 3-4 % in thermally activated SMAs. Actuators will generally need to be replaced following each mission.

Input Energy & Power

REMUS is equipped with a 1 kW·hr Lithium Ion cell. Thermally activated SMAs and LCEs as well as conducting polymers and IPMCs all operate at low voltages and with high currents. The low electromechanical coupling of these actuators results in input electrical powers that are ~ 100 × greater than the work output. Although voltages are similar to those used in electromagnetic drive motors, the currents are ~ 100 × larger. The battery drains 100 × faster, and 100 × more power is demanded. Effectively, the battery mass must be increased by two orders of magnitude, and thus these actuator technologies are not practical for this high bandwidth, finite energy supply application.

In ferroelectrics and dielectric elastomers in particular DC-DCs converter will be required. It remains to be determined how much space this will occupy over and above the cell. Energy recovery circuitry may also be required to obtain reasonable efficiencies and mission lengths in these actuators, as well as in magnetostrictive materials.

Results

Based on preliminary design considerations, ferroelectric polymers and possibly dielectric elastomers are the most promsing technologies, providing the necessary high voltages can be generated.

ACKNOWLEDGMENT

This project was conceived by Dr. Promode Bandyopadhyay and Dr. Harold Bright at ONR. Many thanks to Franzi Tschurtschenthaler for assistance with dielectric elastomer figures of merit.